Field measurements of unsteady friction effects in a trunk transmission pipeline

Mark Stephens, Angus R. Simpson, Martin F. Lambert and John P. Vítkovský

School of Civil and Environmental Engineering, University of Adelaide, South Australia 5005, Australia; PH +61 8 8303 5135; FAX +61 8 8303 4359;
email : mstephen@civeng.adelaide.edu.au

1 ABSTRACT

The relative importance of unsteady friction effects in real pipelines remains a matter of debate. This paper presents the results of a set of field transient measurements on a 13.5 km long trunk transmission water pipeline located in regional South Australia. Modelling has been undertaken using efficient rough pipe turbulent weighting function methods to calculate the unsteady friction contribution. The relative importance of unsteady friction, for no-leak and leak cases, is assessed.

2 INTRODUCTION

Researchers have developed complex models to include unsteady friction effects in transient pipe flow. Some of these models have been verified for single pipelines under laboratory conditions. Nevertheless, persistent questioning of the significance of unsteady friction in field systems continues. While the estimation of the initial pressure rise has been a traditional focus of transient analysis, accurate modelling of transients over longer time periods is becoming increasingly important. For example, a pre-condition to successful inverse transient modelling is an ability to accurately model both the damping and form of a transient as it decays in the longer term.

This paper presents the results of a carefully executed set of field measurements on a full-scale trunk transmission pipeline located near the township of Hanson in regional South Australia. The results of the testing can be generalised to draw conclusions about situations in which unsteady friction modelling may be more or less important.

3 THE HANSON TRUNK TRANSMISSION PIPELINE

3.1 General Details

The trunk transmission pipeline used for the field tests is located near the township of Hanson, in the mid-north country region of South Australia. The “Hanson Trunk Transmission Pipeline” (HTTP) was selected because of its gravity supply tanks, uniformity of pipe material (mild steel cement lined - MSCL) and the possibility of shutting down the main for testing (because a second parallel main was present). The basic layout of the HTTP is shown in Figure 1 :

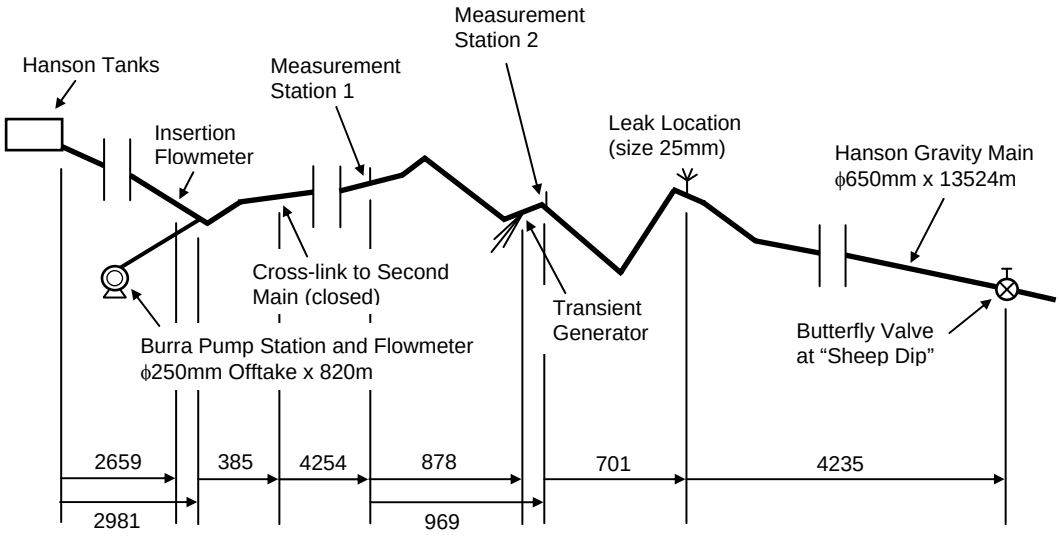

Figure 1 – Layout of the Hanson Trunk Transmission Pipeline (HTTP)

Figures 2 (a) and (b) show the conditions at the upstream (tank) and downstream (isolation valve) ends of the HTTP respectively. Five 9.1 ML tanks connected in series, comprising part of the summit storage at Hanson, formed an upstream boundary condition while a butterfly isolation valve (newly installed) was closed, at a location known as "Sheep Dip", in order to form the downstream boundary condition.

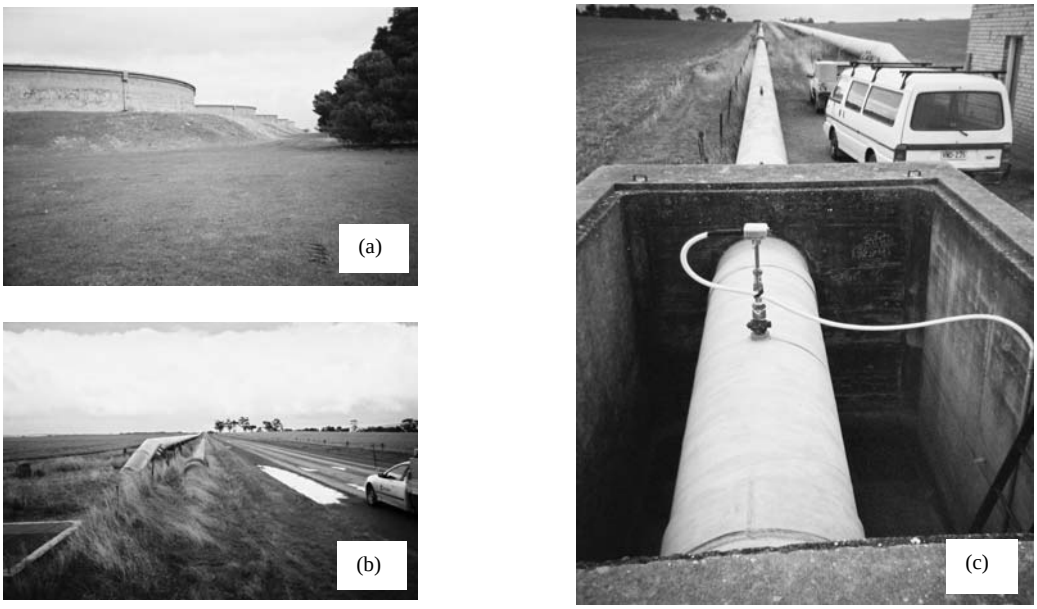

Figure 2 (a), (b) and (c) – Hanson summit storage tanks, "Sheep Dip" butterfly valve location and insertion flowmeter for HTTP

Figure 2 (c) shows the insertion flowmeter in the HTTP identified in Figure 1. Records from this flowmeter indicated that the mean flow in the HTTP was reduced to less than 2 L/s during the test period (when transient tests were not being performed). This small amount of residual leakage can attributed to imperfect sealing of the butterfly isolation valve at "Sheep Dip".

Figures 3 (a) and (b) show the side discharge jet used to generate transients and the leak location respectively. Controlled transients were induced in the HTTP by closing a 50 mm side discharge orifice (over a period of approximately 10 ms). In addition, a leak (25 mm side discharge orifice) was installed on the HTTP (at the location shown in Figure 1) for the purpose of assessing its relative impact on the transient response of the HTTP.

Figure 3 (a) and (b) – Transient generation and leakage on HTTP

The transient response of the HTTP was measured at stations 1 and 2 as shown in Figure 1. Rapid response pressure transducers were installed in existing air valve / fire plugs (AVFPs) at these two locations and pressure response data was recorded at 500Hz.

3.2 Summary of controlled transient tests performed

On the 21st May 2004, a set of 4 controlled transient tests were performed as detailed in Table 1 :

Table 1 – Summary of controlled transient tests

Test No.	Initial flow in main pipe	Initial velocity in main pipe	Burra pump station flow	Leak flow	Initial Reynolds No. for main pipe	Test description
1	45 L/s	0.144 m/s	0 L/s	0 L/s	79,715	No leak test
2	45 L/s	0.144 m/s	0 L/s	0 L/s	79,715	No leak test
3	55 L/s	0.176 m/s	0 L/s	10 L/s	98,043	Leak test
4	55 L/s	0.176 m/s	0 L/s	10 L/s	98,043	Leak test

The flow rate information in Table 1 was obtained from chart records, applicable over the period of the tests, for the flowmeters in the main HTTP and "Burra Pump Station" (as shown in Figure 1). The flow rates from the chart records for the HTTP were checked against the estimated discharge from the generator device using the orifice equation (knowing that a 50mm nozzle had been used with a discharge coefficient of approximately 0.7). The leak discharges were checked as outlined in Section 3.3.

The controlled transients induced by tests 1 and 2, as described in Table 1, resulted in an immediate 75 kPa pressure rise in the HTTP and a maximum pressure rise (above the background steady-state pressure) of approximately 150 kPa (tests 3 and 4 resulted in smaller pressure rises). These pressures were well within the allowable pressure range for the HTTP.

3.3 Estimation of wave speed, pipe roughness and leak characteristics

3.3.1 Wave speed estimation

The HTTP comprises 650 mm diameter MSCL pipe. It is located above ground, supported by concrete pedestals (at approximately 8m spacings) and restrained by full concrete rings at spacings varying from 50 to 100 m. Pipe sections are fully welded.

Plans of the HTTP indicate that it has a wall thickness of 4.8 mm along its entire length. Sections of pipe (previously cut out to be replaced) reveal that the thickness of the cement lining varies between 10 to 15 mm (with an average thickness of approximately 12.5 mm). Following the procedure described by Wylie and Streeter (1993), the theoretical wave speed for the composite steel and cement walled pipe was calculated as approximately 1050 m/s.

Results from the four field tests described in Table 1 indicate that, based on the travel times for the transient wavefronts between the two measurement stations, the wave speed is approximately 1045 m/s (the wavefronts were relatively steep following the 10 ms side discharge closure and could be used to accurately estimate travel times). This value agrees well with the theoretical wave speed.

3.3.2 Roughness estimation

Recent closed circuit camera inspections (CCTV) conducted over a short length of the HTTP near Gum Creek (approximately 300 m of pipeline adjacent to the leak location) suggest that the roughness of the cement lining for that length is less than 2 mm. This is the best available information for the pipeline apart from theoretical information on the likely roughness height of the cement lining in a MSCL pipe. A roughness height of 2 mm has been adopted in the analysis.

3.3.3 Leak characteristics

The leak (shown in Figures 1 and 3 (b)) was installed on the HTTP at the location of an AVFP. An 850 mm long by 55 mm diameter tube was connected to the AVFP and the valve at its base opened to allow a vertical discharge. This base valve has a maximum aperture of approximately 1.5 inches (i.e., 38 mm). However, the base valve was not fully opened so as to control the magnitude of the leak discharge. The geometry of the tube and height of vertical leak discharge were used to estimate the initial vertical velocity of the leak jet and hence a discharge of approximately 10 L/s.

This discharge compared well with that which was calculated using the orifice equation and the knowledge that the AVFP had been opened 6.5 of 10 turns (corresponding to an equivalent orifice opening of approximately 25 mm). Finally, as stated in Table 1, chart records from the insertion flowmeter for the test period confirmed that an additional 10 L/s discharge occurred in the HTTP when the leak was open.

4 MODELLING UNSTEADY FRICTION

A one dimensional weighting function unsteady friction model is used to perform the calculation of unsteady friction in this paper. Zielke (1968) first developed a weighting function type unsteady friction model, for laminar transient pipe flow conditions, utilising past weighted velocity changes to determine unsteady friction loss. This original formulation was restricted to laminar flow conditions until Vardy and Brown (1995) developed weighting functions for smooth pipe turbulent flow conditions. Vardy and Brown (2004) also subsequently developed weighting functions for rough pipe turbulent flow conditions.

Full convolution of the velocity changes with the weighting function, throughout the history of the transient, proved computationally taxing until Trikha (1975) and Kagawa et al. (1983) developed efficient recursive approximations to eliminate the need for convolutions. Vitkovsky et al. (2004) adapted the efficient recursive approximations developed for laminar flow to smooth and rough pipe turbulent flow conditions.

Traditionally, transient flow in pipes is calculated using the fundamental continuity and momentum equations as presented by Wylie and Streeter (1993) :

$$\frac{\partial H}{\partial t} + \frac{a^2}{gA}\frac{\partial Q}{\partial x} = 0 \quad \text{and} \quad \frac{\partial H}{\partial x} + \frac{1}{gA}\frac{\partial Q}{\partial t} + h_f = 0 \tag{1}$$

after convective acceleration and slope terms have been neglected.

The frictional component in the momentum equation, h_f, includes both steady and unsteady friction effects :

$$h_f = h_{fS} + h_{fU} \tag{2}$$

The calculation of the h_{fU} term (i.e., unsteady friction) may be performed using the efficient recursive approximation developed by Kagawa et al. (1983) :

$$h_{fU}(t) = \frac{16\nu}{gD^2}\sum_{k=1}^{N} y_k(t) \tag{3}$$

in which the variables y_k are defined as

$$y_k(t+\Delta t) = e^{-n_k \Delta\tau} y_k(t) + m_k e^{-0.5 n_k \Delta\tau}\left[V(t+\Delta t) - V(t)\right] \tag{4}$$

and the weighting function is approximated by

$$W_{app}(\tau) = \sum_{k=1}^{N} m_k e^{-n_k \tau} \tag{5}$$

Values for the exponential parameters m_k and n_k are determined by fitting to the true weighting function (only needs to be done once). The value of k varies with the value of $\Delta\tau$ (= $4\nu\Delta t/D^2$: the dimensionless time step). The values of y_k need to be stored and updated on an on-going basis.

Vitkovsky et al (2004) adapted the efficient recursive approximation to smooth and rough pipe turbulent flow conditions. The true weighting function developed by Vardy and Brown (1995 and 2004) for these conditions takes the form :

$$W(\tau) = \frac{A^* e^{-B^* \tau}}{\sqrt{\tau}} \tag{6}$$

in which :

$$A^* = \frac{1}{2\sqrt{\pi}} \text{ and } B^* = 0.135\,\mathrm{Re}^{\kappa} \text{ for smooth pipe flow} \tag{7}$$

with $\kappa = \log_{10}(14.3\mathrm{Re}^{-0.05})$

and

$$A^* = 0.0103\sqrt{\mathrm{Re}}\left(\frac{\varepsilon}{D}\right)^{0.39} \text{ and } B^* = 0.352\,\mathrm{Re}\left(\frac{\varepsilon}{D}\right)^{0.41} \text{ for rough pipe flow} \tag{8}$$

Vitkovsky et al. (2004) followed a similar procedure to that adopted by Kagawa et al. (1983) in order to fit an approximate weighting function. However, in the case of

turbulent flow, the magnitude of the coefficients A^* and B^* are dependent upon the Reynolds number of the flow (and hence the initial conditions) and the relative roughness of the pipe(s). Vitkovsky et al. (2004) overcame this problem by scaling the fitted values of the exponential parameters m_k and n_k (again, this fitting only needed to be undertaken once) using values of A^* and B^* determined for each pipe initial condition or roughness :

$$W^*_{app}(\tau) = \sum_{k=1}^{N} m^*_k e^{-n^*_k \tau} \tag{9}$$

in which :

$m^*_k = m_k / A^*$ and $n^*_k = n_k - B^*$ are the scaled exponential parameters

Values of m_k and n_k, determined for laminar and turbulent flow conditions, can be obtained from Vitkovsky et al. (2004). These values have been implemented, in an efficient recursive approximation for the calculation of unsteady friction under laminar and turbulent (smooth and rough pipe) flow conditions, for the following analysis.

5 COMPARISONS BETWEEN THE MEASUREMENTS AND MODELLING

A 1-D Method of Characteristics (MOC) transient model, modified to allow the calculation of unsteady friction under laminar and turbulent (smooth and rough pipe) flow conditions, is used in the analysis. The HTTP has a roughness height of approximately 2 mm and the test flows were in the transition turbulent section of the Moody diagram. Consequently, the unsteady friction calculations are performed using the equations applicable to turbulent flow conditions in a rough pipe.

The HTTP (total length of 13,524 m) is discretised into 644 sub-pipe segments (each 21 m long). A uniform wave speed of 1050 m/s is applied giving a time step in the calculations of 0.02 seconds. A background flow rate of 2 L/s, discharging through the "Sheep Dip" butterfly valve (as identified in Section 3.1), has been included. The “Burra Pump Station” off-take has also been included such that additional reflections associated with it are properly modelled.

5.1 No-leak test results and modelling

Figures 4 (a) and (b) and 5 (a) and (b), for measurement stations 1 and 2 respectively, illustrate that there is a considerable improvement in the accuracy of the model when rough pipe turbulent unsteady friction is included for the no-leak tests. The relative effects of unsteady friction on the overall head loss during the transient, and on the shape of the response, are assessed, for the no-leak case, in Section 6.

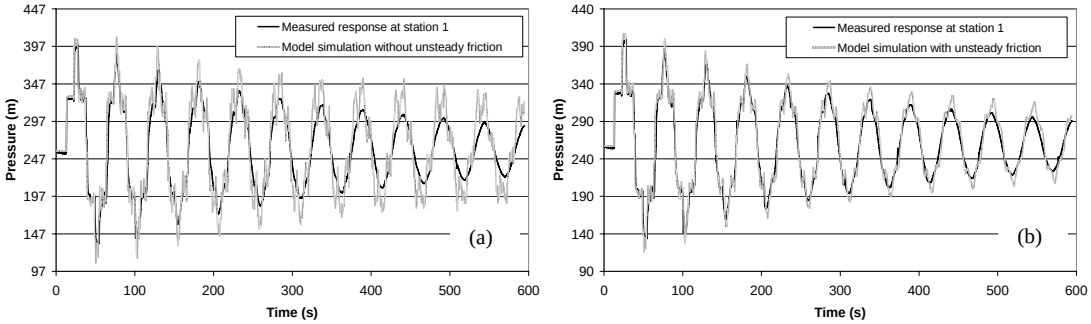

Figure 4 (a) and (b) – Comparison of measured and modeled responses at station 1 (no-leak) when unsteady friction is and is not included in the model

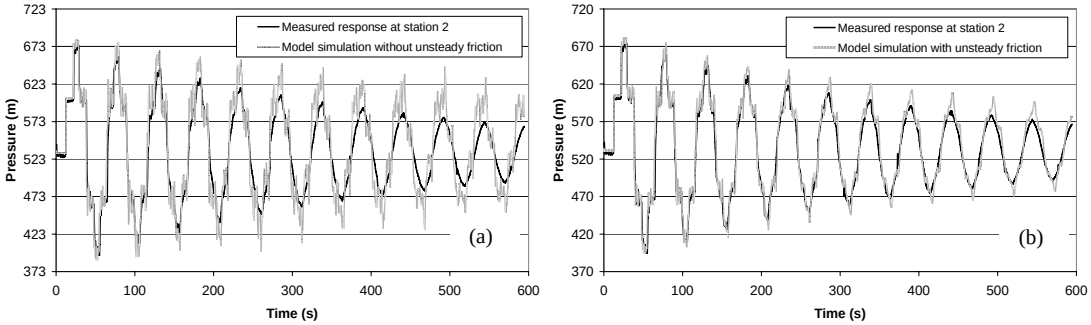

Figure 5 (a) and (b) – Comparison of measured and modelled responses at station 2 (no-leak) when unsteady friction is and is not included in the model

5.2 Leak test results and modelling

Figures 6 (a) and (b) and 7 (a) and (b), for measurement stations 1 and 2 respectively, also indicate an improvement (less than for the no-leak case) in the accuracy of the model when rough pipe turbulent unsteady friction is included for the leak tests. The relative effects of unsteady friction on the overall head loss during the transient, and on the shape of the response, are assessed, for the leak case, in Section 6.

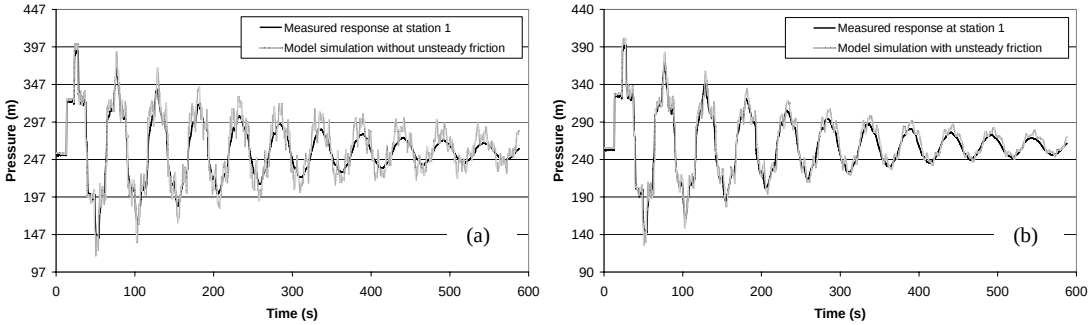

Figure 6 (a) and (b) – Comparison of measured and modelled responses at station 1 (10 L/s leak) when unsteady friction is and is not included in the model

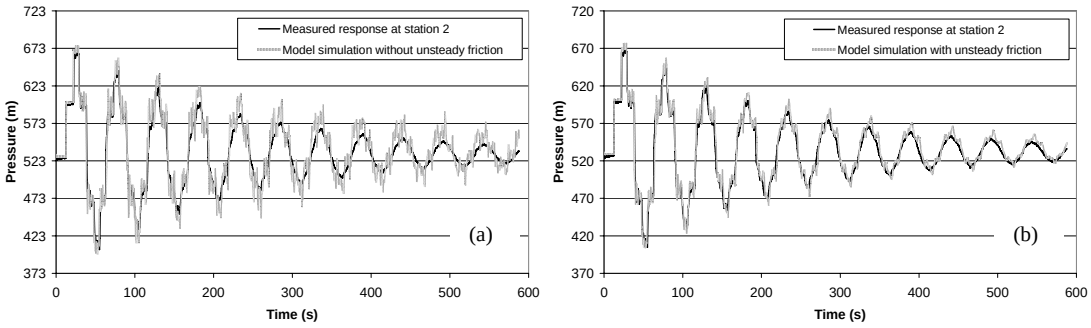

Figure 7 (a) and (b) – Comparison of measured and modelled responses at station 2 (10 L/s leak) when unsteady friction is and is not included in the model

All figures, in both Sections 5.1 and 5.2, show distortions in the modelled transient form (i.e., small peaks and troughs) that are not reflected in the measurements. While unsteady friction greatly improves the comparison between modelled and measured responses, it does not dissipate these distortions. The "Burra Pump Station" off-take is one source of dissipation that has been included in the model. However, two other short lateral sections of 650 mm diameter pipe (less than 10 m long each) have been neglected. Their inclusion in the model may have helped dissipate the distortions.

6 THE RELATIVE IMPORTANCE OF UNSTEADY FRICTION

6.1 Relative importance in the context of overall head loss

The total head variation during the transients has been calculated by taking the sum of the absolute head variations from the initial steady-state pipeline pressure for the no-friction, steady friction and unsteady friction cases (no-leak and leak configurations). These total head variations have then been used to calculate the additional percentage head loss occurring, relative to the no-friction case, when steady friction and then unsteady friction are included (using the results from Sections 5.1 and 5.2) as shown in Table 2 :

Table 2 – Percentage (%) overall head loss for no-friction, steady friction and unsteady friction models (for no-leak and leak tests)

Model	No-leak tests			Leak tests (10 L/s)		
	Station 1	Station 2	Avg.	Station 1	Station 2	Avg.
No-friction	0.0	0.0	0.0	39.1	39.4	39.3
Steady friction	23.4	23.4	23.4	51.4	51.9	51.7
Unsteady friction	32.8	33.2	33.0	56.9	57.4	57.2

For the no-leak tests, Table 2 illustrates that 23.4% of the overall head loss during the transient is due to the contribution of steady friction. However, steady friction does not account for all the observed head loss as shown in Figures 4 (a) and 5 (a) in

Section 5.1. The inclusion of unsteady friction is required to improve the match between the measured and predicted responses for the no-leak case as shown in Figures 4 (b) and 5 (b). The inclusion of unsteady friction increases the overall head loss to 33.0% of which 9.6% is due to unsteady friction.

For the leak tests, Table 2 illustrates that 39.3% of the overall head loss during the transient is due to the contribution of the leak (the leak is 10 L/s and represents approximately 18% of the 55 L/s base flow in the HTTP). Once steady friction is included in the model, the overall head loss increases to 51.7% with 12.4% attributable to steady friction. However, the leak and steady friction do not account for all the observed head loss as shown in Figures 6 (a) and 7 (a) in Section 5.2. The inclusion of unsteady friction is required to improve the match between the measured and predicted responses for the leak case as shown in Figures 6 (b) and 7 (b). The inclusion of unsteady friction increases the overall head loss to 57.2% of which 5.5% is due to unsteady friction.

6.2 Relative importance in the context of shape and form of transient

While the percentages of overall head loss provide one measure of the influence of unsteady friction, objective function comparisons provide another measure more relevant to the shape of the modelled transients. The objective function is calculated as the sum of the squares of the errors between the measured and modelled responses.

Table 3 lists the percentage improvement in objective function obtained when unsteady friction is included in addition to steady friction in the model. For the no-leak case there is a 71.0% improvement while for the leak case there is a 56.5% improvement. These improvements are illustrated in Figures 4 (b), 5 (b), 6 (b) and 7 (b) in Sections 5.1 and 5.2.

Table 3 – Percentage (%) improvement in objective function from steady friction to unsteady friction model (for no-leak and leak tests)

Test case	Station 1	Station 2	Average
No leak	71.7	70.3	71.0
Leak (10 L/s)	56.6	56.4	56.5

The objective function is also the measure by which inverse transient modelling is performed. Without the inclusion of unsteady friction, the objective function will include large errors. These errors are sufficient to prevent the use of inverse transient analysis to identify the presence, in this field study, of the 10 L/s leak.

7 CONCLUSIONS

While the field tests performed on the HTTP were specific, broader conclusions can be drawn about the relative importance of unsteady friction. For both no-leak and leak cases, the inclusion of unsteady friction considerably improved the performance of the transient model. However, the Reynolds numbers for the tests were relatively low and conducive to unsteady friction effects. Under conditions with higher Reynolds numbers, the effect of unsteady friction is reduced.

The results also confirm that the effect of unsteady friction decreases when leak damping is present. The leak size was sufficient to reduce the influence of unsteady friction from 9.6% to 5.5% (as gauged using the measure of relative overall head loss). Nevertheless, the inclusion of unsteady friction modelling was warranted and is particularly important if inverse transient modelling is to be used to detect leakage. More research (both numerical and in the field) is required to continue to identify the circumstances in which unsteady friction is important when modelling transients.

8 ACKNOWLEDGEMENTS

The writers would like to acknowledge the support and assistance received from SA Water Corporation staff in carrying out the field tests. The writers also acknowledge the financial support received from the Australian Research Council.

9 REFERENCES

(1) Kagawa, T., Lee, I., Kitagawa, A. and Takenaka, T. (1983) “High Speed and Accurate Computing Method of Frequency-Dependent Friction in Laminar Pipe Flow for Characteristics Method” *Transactions of the Japanese Society of Mechanical Engineers*, 49(447), 2638-2644

(2) Trikha, A. (1975) “An Efficient Method for Simulating Frequency-Dependent Friction in Transient Liquid Flow” *Journal of Fluids Engineering*, Transactions of the ASME, 113(4), 569-573

(3) Vardy, A. and Brown, J. (1995) “Transient, Turbulent, Smooth Pipe Friction” *Journal of Hydraulic Research*, IAHR, 33(4), 435-456

(4) Vardy, A. and Brown, J. (2004) “Transient Turbulent Friction in Fully-Rough Pipe Flows” *Journal of Sound and Vibration*, 270, 233-257

(5) Vitkovsky, J., Stephens, M., Bergant, A., Lambert, M. and Simpson, A. (2004) “Efficient and Accurate Calculation of Zielke and Vardy-Brown Unsteady Friction in Pipe Transients” *9th International Conference on Pressure Surges*, BHR Group, Chester, UK

(6) Wylie, E.B. and Streeter, V.L. (1993) Fluid Transients in Systems, Prentice-Hall Inc., Englewood Cliffs, New Jersey, USA

(7) Zielke, W. (1968) “Frequency-Dependent Friction in Transient Pipe Flow” *Journal of Basic Engineering*, Transactions of the ASME, 90(1), 109-115

10 NOTATION

a = wave speed
A = pipe cross-section area
A^*, B^* = Vardy-Brown weighting function coefficients
D = pipe diameter
g = gravitational acceleration
h_f = friction head loss
h_{fS} = steady friction head loss
h_{fU} = unsteady friction head loss
H = head
m_k, n_k = exponential sum coefficients
m_k^*, n_k^* = scaled exponential sum coefficients
N = number of exponential terms
Q = flow rate
Re = Reynolds number
t = time
V = average velocity
W = true weighting function
W_{app} = approximate weighting function
x = distance
y_k = efficient method coefficient
ε = pipe wall roughness
ν = kinematic viscosity
τ = dimensionless time